Check for updates

Unidirectional transport of water nanodroplets entrapped inside a nonparallel smooth surface: a molecular dynamics simulation study†

Awais Mahmood, [ID] [a] Shuai Chen, [ID] [b] Lei Chen,[a] Dong Liu, [ID] [a] Chaolang Chen,[a] Ding Weng[a] and Jiadao Wang*[a]

The unidirectional transport of liquid nanodroplets is an important topic of research in the field of drug delivery, labs on chips, micro/nanofluidics, and water collection. Inspired by nature a nonparallel surface (NPS) is modelled in this study for pumpless water transport applications. The dynamics of water transport is analyzed with the aid of Molecular Dynamics (MD) simulations. There were five different types of NPSs namely A1, A2, A3, A4, and A5 utilized in this study, with separation angles equal to 5°, 7°, 9°, 11°, and 13° respectively. The water droplet was placed at the beginning of the open end of the NPS and it moved spontaneously towards the cusp of the surface in all cases except for the 13° NPS. The size of the water droplet, too, was altered and four different sizes of water droplets (3000, 4000, 5000, and 6000 molecules) were utilized in this study. Furthermore, the surface energy parameter of the NPS was also changed and four different values, *i.e.* 7.5 eV, 17.5 eV, 27.56 eV, 37.5 eV were assigned to the surface in order to represent a surface with hydrophobic to hydrophilic characteristics. In addition the importance of water bridge formation for its spontaneous propulsion with the influence of surface energy and droplet size is also discussed in this study. Moreover, a unique design is modelled for the practical application of water harvesting and a large size water droplet is formed by combining two water droplets placed inside a NPS.

1. Introduction

The pumpless, unidirectional transport of a liquid droplet has become an interesting topic of research in recent years due to its abundant presence in nature and broad practical applications. In the field of micro/nanofluidics and practical applications like lab-on-a-chip devices, a directed motion is highly desired to transport substances suspended in the liquid droplet.[1,2] Plenty of techniques have been employed for droplet propulsion inside the solid surface and the most common of those are, electrowetting,[3,4] thermal gradients,[5] vibrating substrates,[6,7] vapor driven techniques,[8] and oscillatory electric fields.[9] Moreover, surfaces with wettability gradients and surfaces with an unsymmetrical structure can usually efficiently aid the unidirectional motion of the liquid.[10,11] However, the transport of the liquid droplet in the above

State Key Laboratory of Tribology, Tsinghua University, Beijing, 100084, China. E-mail: jdwang@mail.tsinghua.edu.cn; Tel: +86-10-62796458

*Institute of High Performance Computing, A*STAR, 138632, Singapore*

† Electronic supplementary information (ESI) available: Movie of the equilibrium states of water droplet on NPS having different separation angle. This movie demonstrates the bridge formation mechanism and the transport mechanism of water nanodroplet in which white, red, and cyan spheres represent the hydrogen, oxygen and NPS atoms, respectively (ZIP). See DOI: 10.1039/c9ra08968c

mentioned studies is dependent on an external source or on the surface heterogeneity.[12]

In a number of industrial processes, it has been observed that a bridge of liquid is formed between two solid surfaces. In the case of offset printing the ink is transferred between the rollers by continuous stretching and breaking of the ink bridges.[13,14] Many studies have been conducted regarding the stability of the liquid bridge but most of them were focused on axisymmetric liquid bridges between two parallel surfaces.[15,16] In nature, it has been evident that the liquid bridges can also be formed between two nonparallel surfaces (NPSs) such as phalarope and other shore birds which form a liquid bridge in between their nonparallel beaks for trapping prey.[17] It has been reported that instability may occur when the two surfaces are nonparallel and the bridge of liquid between them may propel itself towards the cusp of two solid surfaces.[18] The spontaneous unidirectional motion of liquid droplet triggered by instability may have plenty of practical applications. Such phenomena can be helpful for water harvesting induced by condensation,[19] to transport liquid droplets in micro/nano fluidic systems[20] and to produce a liquid drop of a desired size.[21]

The spontaneous propulsion of liquid droplets bridged between NPSs is usually observed in hydrophilic surfaces but the underlying physical principal of such a phenomenon is still not clear.[22] In one of the studies it was observed that the

dihedral angle of two NPSs plays a crucial role in deciding the stability of the liquid bridge. It has been reported that when the dihedral angle exceeds a critical range the bridge is no longer stable and propels itself towards the cusp of the surface.[23] The computer aided simulations namely molecular dynamics (MD) simulations provide a powerful tool in understanding the solid–liquid interactions at nanoscale and could be useful to understand the liquid bridge formation and propulsion mechanism between the NPSs at nanoscale. In one of recent studies the efficient transport between disjoint nanochannels by a water bridge is studied in details with the aid of MD simulations.[37] In another study the MD simulations of water nanodroplet bridged between two parallel surfaces is conducted but an external forces is applied to mimic the stretching and squeezing of the phalarope bird beak.[24]

Even though a number of experimental and analytical studies have been conducted on the aforementioned topic, but to best of author's knowledge a detailed analysis of water droplet bridged between two NPSs at nanoscale has not been reported yet. In order to understand the spontaneous transport of the droplet towards the cusp of the surface a virtual solid surface having distinct lattice structure may be utilized to model the solid surface.[25,26] The surface wettability of the solid surface can be altered from hydrophobic to hydrophilic by adjusting its potential parameter.[27] The movement of the droplet can be observed visually and its displacement at each time step could be calculated in order to understand the spontaneous movement of the liquid droplet.[28]

In this study, the unidirectional propulsion of the water nanodroplet bridged between two nonparallel solid surfaces is analyzed. In addition, the effect of the surface angle between two nonparallel surfaces, the size of water droplet and the wettability of the solid surface on the spontaneous motion of water droplet is also analyzed in this study. This study provides the fundamental understanding about the pumpless propulsion of water nanodroplet bridged between solid NPSs.

2. Methods

A nonparallel solid surface (NPS) having different separation angle is modeled and a water droplet is placed at the edge of the bottom strip in between two NPSs, as shown in Fig. 1. The solid surface is modeled by utilizing a simple cubic structure with a lattice constant, a, which is kept equal to 3 Å.[29] The solid surface contains four homogeneous layers of atoms having 3 Å distance between each layer. The simple point charged potential water model (SPC/E) is utilized in this simulation study where each water molecule consist of two hydrogen atoms with +0.4238e and one oxygen atom with −0.8476e charge.[30] The bond angle between H–O–H atoms was kept equal to 109.47° while the bond length of O–H atoms was kept equal to 1 Å. The angle and bond length of water molecules were fixed by SHAKE algorithm.

In order to observe the pumpless propulsion of water droplet under the influence of solid surface geometry, five different types of NPSs have been modeled based on the surface angle difference as shown in Fig. 1. The surface angle "θ" of the NPS is

altered from 5° to 13° by an increment of 2° but the length "L" and width "W" of the NPS is kept constant for all five types which is equal to 300 Å, and 150 Å, respectively, as shown in Fig. 1a. The thickness of the solid surface is 12 Å (4 atoms thick) and the separation distance "S" depends on the surface angle of the NPS, the detailed information about this is listed in the Table S1.† In addition, the energy parameter of the solid surface is altered in order to analyze the effect of hydrophobic and hydrophilic characteristics of solid surface on the transport mechanism of the water nanodroplet. Furthermore, a water droplet is placed at open end of the nonparallel surface having a distance of 3 Å between the solid and liquid atoms. The water molecules were initially in a 3D space and represent a regular state where each molecule was 3 Å away from each other.[31] In order to observe the influence of the size of droplet on the spontaneous transportation of water droplet, four different size of water droplet were utilized in this study having $N = 3000$, 4000, 5000 and 6000 molecules as shown in Fig. 1. It is evident from the previous studies that, in order to minimize the computation cost and to improve the calculation efficiency of the simulation model the gas molecules are not considered in this study.[32,33]

In this study the intermolecular interaction forces between the water molecules is represented by the combination of electrostatic interaction and calculated by Coulomb's law. In addition, the dispersion and repulsion forces were measured by the aid of Lennard-Jones (L-J) potential.[34]

$$U_{ij} = 4\varepsilon_{ij}\left[\left(\frac{\sigma_{ij}}{r_{ij}}\right)^{12} - \left(\frac{\sigma_{ij}}{r_{ij}}\right)^{6}\right] + \frac{Cq_iq_j}{\varepsilon_o r_{ij}}, \ \ r_{ij} < r_c \qquad (1)$$

As mentioned above the subscripts i and j represent oxygen (O), hydrogen and NPS (solid surface) atoms. Moreover, the charges on the atoms are represented by q_i and q_j while σ_{ij} and ε_{ij} represent the distance where the depth of the potential well and the interatomic potential is zero. In addition, r_{ij} represents the distance between the two atoms and r_c represents the cutoff potential. The ε_o represent the dielectric constant and it is set to be equal to 1.0. The cutoff potential in this study is kept equal to 15 Å which means $U_{ij} = 0$ when $r_{ij} \geq 15$ Å. The Lorentz–Berthelot mixing rule is utilized to calculate the interatomic mixed-atom potential.[35]

$$\sigma_{ij} = \frac{\sigma_{ii} + \sigma_{jj}}{2} \qquad (2)$$

$$\varepsilon_{ij} = \sqrt{\varepsilon_{ii} \times \varepsilon_{jj}} \qquad (3)$$

The energy parameter ε_{ij} of oxygen atoms and hydrogen atoms is set to be 6.48 meV and 0 meV, while the energy parameter of the nonparallel surface is altered from 7.5 meV to 37.5 meV. In addition, the value of σ_{ij} for water and solid (NPS) surface is kept equal to $\sigma_{o-o} = 3.166$ Å and $\sigma_{s-s} = 3.826$ Å, respectively. Furthermore, a flat solid surface of uniform wettability is modeled to analyze the contact angle of 3000 water molecule droplet and the contact angle is measured at four different energy parameters in order to represent a surface with hydrophobic to hydrophilic characteristics.
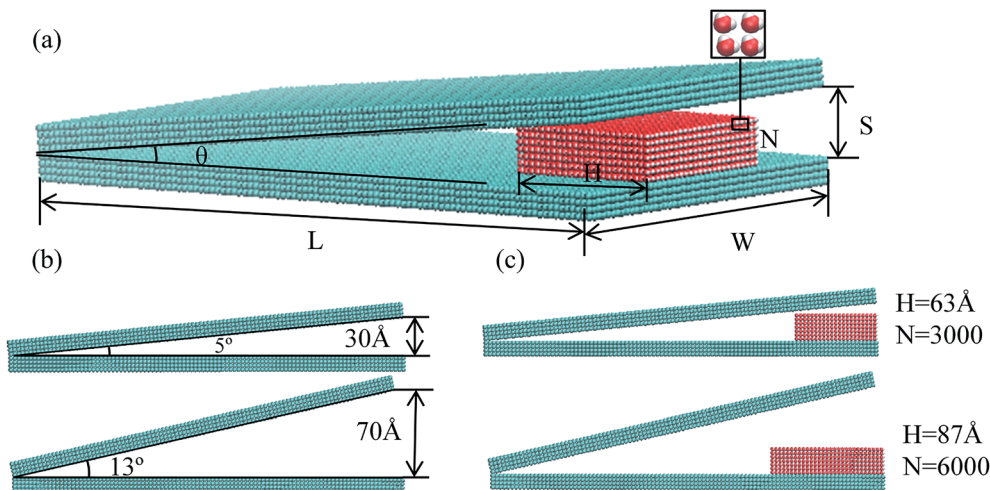
Fig. 1 Initial structure of the ensemble containing (a) nonparallel surface made by simple cubic atomic structure and water molecules placed at the edge of the open end of the surface (b) five different types of nonparallel surfaces based on the separation distance "S" and the surface angle "θ" (c) four different size of water droplet having number of molecules "N" equals to 3000, 4000, 5000, and 6000.

All the simulations were carried under periodic boundary condition with fixed number, volume, and temperature (NVT) ensemble in LAMMPS molecular dynamics (MD) software.[36] All the simulations were run for two nano seconds (2.0 ns) duration. The integration time step for all the simulation models was kept equal to 1 fs. The particle–particle particle–mesh (PPPM) algorithm is utilized to estimate the long-range electrostatic interactions among the water molecules only and its precision value is set to be equal to 10^{-5}. The temperature of the water droplet was fixed at 300 K with the aid of Nose–Hoover thermostat. The lateral size of the solid surface is seven times more than the water cube. In addition, the dimension of the simulation box was kept ten times higher than the size of water droplet so that the influence of molecules in the duplicate domain on the behavior of the droplet could be neglected. Furthermore, the position of the substrate is set stationary and it represent as an inert wall. It was observed that the temperature of water droplet was stayed steady and a deviation of less than 5.0 K is observed during the whole simulation time.

In this study, a two-step method is utilized to calculate the velocity of the water droplet on NPS surface. Firstly, mean square displacement (MSD) data of water molecules calculated at each time step is extracted from simulation results. Secondly, to acquire the velocity of the droplet at each time step the square root of the difference of two consecutive MSD data is divided by the simulation time step (1.0 fs). To calculate the average velocity during 2.0 ns duration of simulation the average velocity at each time step is summed up and divided by the total number of time steps in during this duration. Secondly, four different sizes, *i.e.* 3000, 4000, 5000 and 6000 water molecule droplets were utilized to observe the influence of size of water droplet on its unidirectional transport. Thirdly, the surface energy parameter (L-J Potential) of the NPS (solid surface) is set equal to (7.5 meV, 17.5 meV, 27.5 meV, and 37.5 meV) to obtain a surface with different wettability, and its center of mass (COM) data is measured throughout the simulation

time at each defined energy parameter. Furthermore, water droplet contact angle on flat surface is also measured at above mentioned energy parameter condition. At last, the spontaneous transport of water droplet is observed on different types of surfaces having different surface angle or separation distance. In addition, a solid surface inspired by the nonparallel structure is modeled in this study in order to collect two water nanodroplets confined inside the NPS. The COM and average velocity data, of both water droplets, is measured during the 2.0 ns simulation time. Moreover, the importance of the bridge formation in unidirectional transport of water nanodroplet is also addressed in this study. The water droplet trapped inside a NPS move towards the cusp of the surface is due to the existence of bridge which is essential for water transportation.

3. Results and discussion

3.1 Unidirectional transport of water on different types of NPS

The unidirectional transport of water nanodroplet is observed when it is placed on bottom surface at the open end of the nonparallel surface (NPS). The NPS is modeled with cubic atomic structure with smooth surface as shown in Fig. 1a. To analyze the effect of surface angle "θ" on the movement of the nanodroplet the energy parameter of the NPS is kept equal to 17.5 meV. Five different NPSs namely A1, A2, A3, A4, and A5 having surface angle equal to 5°, 7°, 9°, 11°, and 13° respectively are modeled and their effects on water transport are analyzed in this study as shown in Fig. 1b. The reason behind selection of only these five surface angles is due to the water nanodroplet bridge formation dependence on the surface angle. When the surface angle is too big, *i.e.* beyond 13°, then the water nanodroplet could not touch the top surface of the NPS, and hence there is no bridge formation, which results in stationary droplet attached to the bottom of the NPS. It has been found that the surface angle has a considerable influence on the pumpless propulsion of water nanodroplet. The A1 and A5 NPSs are

shown in the Fig. 1b. The results reveal that the average velocity of water nanodroplet on NPS surface is higher on the surface having large surface angle and it is maximum in case of A4 and there is no bridge formation in A5 NPS because of its larger surface angle. In this case, the water droplet contains 6000 molecules and its size is kept same for all types of NPSs. The COM data at each time step is recorded for 2 ns simulation time and it is plotted as shown in Fig. 2a. It is evident that the water droplet has highest displacement on A4 surface and it is lowest in A1 NPS.

The center of mas (COM) data along the x-axis is plotted in Fig. 2a. The COM function in LAMMPS calculated the center-of-mass of the group of atoms, including all effects due to atoms passing thru periodic boundaries. A vector of three quantities is calculated by utilizing this compute function, while in this study the droplet is transported in one direction which is along x-axis so the data along this axis is plotted and analyzed.

It has been revealed that the velocity of the droplet is highest for A4 NPS while, due to no bridge formation the droplet could not move towards the cusp of the NPS and hence, there is no droplet transport in A5 NPS. It can be concluded that for efficient droplet transport confined inside the NPS it is necessary that the water droplet should touch both top and bottom surfaces of the substrate and create a liquid bridge. This liquid bridge formation is essential for droplet transport as it can be

seen in Fig. 3 and 4. The pumpless propulsion of the nanodroplet is mainly dependent on the surface angle and, it should be tuned in a manner which aid in efficient transport of the nanodroplet. For the NPS with smaller surface angle, spontaneous propulsion of water nanodroplet is also observed but it is less efficient than the surface with larger surface angle or separation distance.

The maximum average velocity of water nanodroplet is found over A4 surface which is equal to 13.3 nm ns^{-1} and the minimum average velocity of water nanodroplet is found over A1 surface which is equal to 8.1 nm ns^{-1}. The COM results further confirm that the droplet move farthest in case of A4 NPS as hence has the highest average velocity of on its surface.

The mechanism behind this pumpless propulsion of water nanodroplet can be explained by the aid of interaction energy data of 6000 water molecule droplet on five different NPSs. The data is plotted in Fig. 3 and it can be seen that the interaction energy between the water molecules and A1 NPS (solid surface) is lowest among all the cases. The lower interaction energy results in low velocity while the interaction energy is highest in case of A4 NPS which result in highest average velocity over the course of whole simulation. The interaction energy data of A5 NPS does not decay during the simulation time which further confirms that there is no bridge formation in this case which result in a stationary water droplet and no transportation. The other reason for this spontaneous propulsion could be linked to the contact angle hysteresis, as the water nanodroplet is attached with the top and bottom surface of the NPS it will cause difference in advancing and receding contact angle of water droplet aiding towards the spontaneous propulsion of water droplet.

It can be seen in Fig. 4 that water nanodroplet confined inside the NPS result in spontaneous propulsion of liquid droplet in all the cases except for A5 NPS where there is no bridge formation occurred. It is evident that the transport of liquid is highest in case of A4 with largest distance covered while it is lowest in case of A1. For efficient propulsion of water nanodroplet in real applications, the surface angle should be designed carefully and in accordance to the water droplet size.
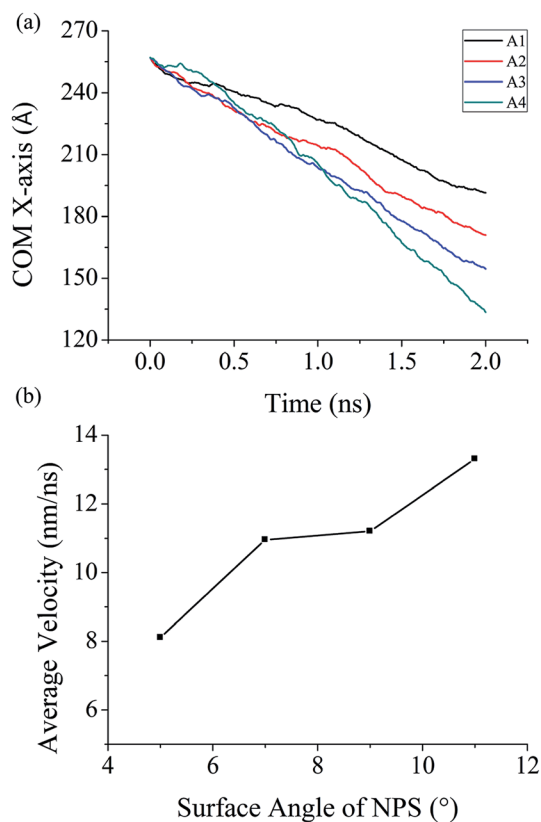

Fig. 2 Simulated results of (a) COM data of 6000 water molecules on different types of NPS (b) average velocity of 6000 water molecules on different types of NPS.
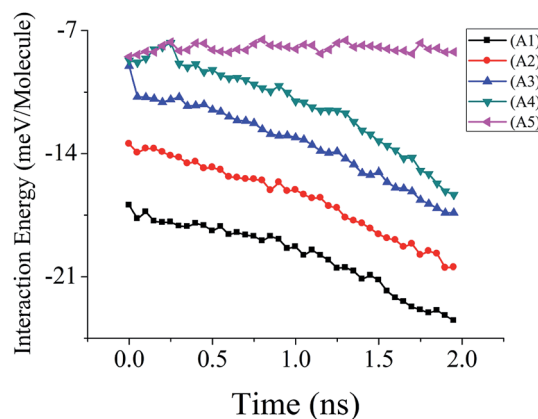

Fig. 3 Interaction energy data of 6000 molecules water droplet confined inside five different types of NPS.
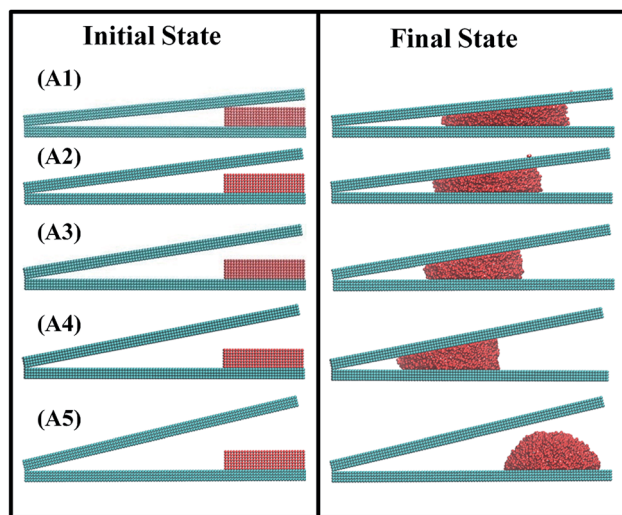
Fig. 4 Ensemble containing 6000 water molecules (a) initial state with (i, ii, iii, iv, and v) represent A1, A2, A3, A4, and A5 NPS (b) final state of the ensemble after 2 ns simulation time.

3.2 Unidirectional transport of water on NPS with different droplet size

In this study, the effect of droplet size on the unidirectional propulsion of water nanodroplet over NPS is analyzed. For this purpose, total four different sizes of water droplets were utilized, containing 3000, 4000, 5000 and 6000 molecules. The average velocity of the unidirectional transport of water droplet over solid NPS is measured for 2.0 ns simulation time. The energy parameter of the NPS was kept equal to 17.5 meV for all sizes of water droplets while the COM and average velocity for each case was recorded and plotted in Fig. 5. Furthermore, different sizes of water droplet were placed on NPSs having different surface angle and the results are also plotted in Fig. 5.

The results reveal that the average velocity of larger water droplet is higher than the smaller water droplet in all cases. Moreover, the average velocity is highest when both surface angle and number of water molecules is highest, while it is lowest when surface angle and number of water molecule is lowest. It can be concluded that for the faster transport of water droplet it is necessary to have a larger surface angle between two NPSs. Furthermore, it is evident that smaller droplet has comparatively lower average velocity over the course of spontaneous propulsion than the larger droplet and the trend is similar in all types of NPSs.

The maximum average velocity of water droplet containing 6000 molecules was found over A4 NPS and it was calculated to be around 13.3 nm ns^{-1}. The minimum velocity was measured over the A1 NPS and it was around 6.25 nm ns^{-1} containing 3000 water molecules. Similarly, the maximum average velocity of 4000 molecules water droplet was calculated around 10.74 nm ns^{-1} over A4 NPS while its minimum velocity was measure around 6.47 nm ns^{-1} over A1 NPS. Also, for the 5000 molecule water droplet the maximum average velocity was measured around 11.51 nm ns^{-1} over A4 NPS and its minimum velocity was around 7.02 nm ns^{-1} over A1 NPS. These findings
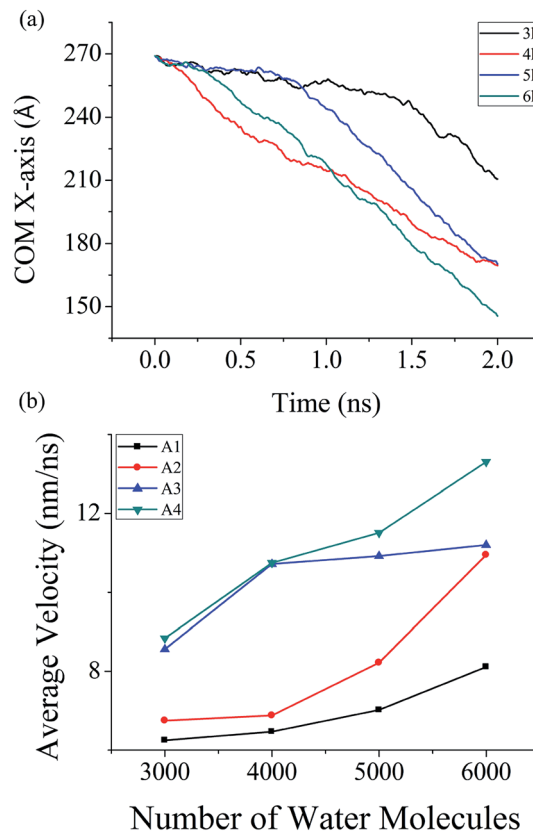

Fig. 5 Simulated results of 3000, 4000, 5000 and 6000 water molecules. (a) COM data on A4 NPS (b) average velocity on four different types of NPS.

further confirm that the A4 NPS transport water droplet at a higher velocity as compared to other four surfaces due to large bridge angle formation which aid in higher transportation rate. In addition, the large water nanodroplet possesses high transport characteristics due to the fact that larger droplets can form a stronger bridge between the NPS. For efficient transportation of water nanodroplet, it is necessary that the solid surface should have such type of geometrical structure (surface angle) which aid in higher rate of water propulsion. Inspired by the spontaneous propulsion mechanism of the NPS, a structure is designed to collect two water nanodroplets confined inside a NPS. In Section 3.4, a structure having dual NPS is designed to collect two water droplets and the results are plotted to further understand the phenomena behind this propulsion of water droplet.

3.3 Unidirectional transport of water on NPS with different surface wettability

In order to investigate in detail the effect of surface wettability on the unidirectional transport of water droplet on the NPS four different energy parameter values has been selected, i.e. 7.5 meV, 17.5 meV, 27.5 meV, and 37.5 meV, this provides a surface with characteristics ranging from hydrophobic to hydrophilic. The average velocity data is measured on each type of NPS with each surface energy parameter and the data is plotted in Fig. 6b.

In this case, a water droplet containing 4000 water molecules is utilized to observe the effect of surface wettability on its propulsion. The COM data of 4000 molecules water droplet on A1 NPS is also measured in this study and plotted in Fig. 6a. It is revealed that when the energy parameter is high, *i.e.* the surface is hydrophilic and the average velocity of the droplet is comparatively higher than that on hydrophobic surface provided the condition that there is a stable water droplet bridge formation between the two NPSs.

As shown in Fig. 6b, the average velocity of water droplet is high on surface with strong surface wettability and large separation angle. The maximum average velocity of water droplet was equal to 12.66 nm ns^{-1} in case A4 NPS having surface energy equal to 7.5 meV. This case is an exception where there is a water bridge formation occur inside A5, the reason behind this is linked to the high contact angle (110.5°) which result in bridge formation between the A5 NPS. Furthermore, the minimum average velocity was measured around 6.29 nm ns^{-1} over the A1 NPS having surface energy equal to 7.5 meV. Furthermore, it can be seen in Fig. 6a that the COM data of water droplet on A1 surface shows high transportation rate on surface with strong surface wettability (hydrophilic) and it is low on the surface with low surface energy (hydrophobic). The COM results show similar trend as exhibited before and it further confirms that the stronger surface wettability aid in faster droplet transport.
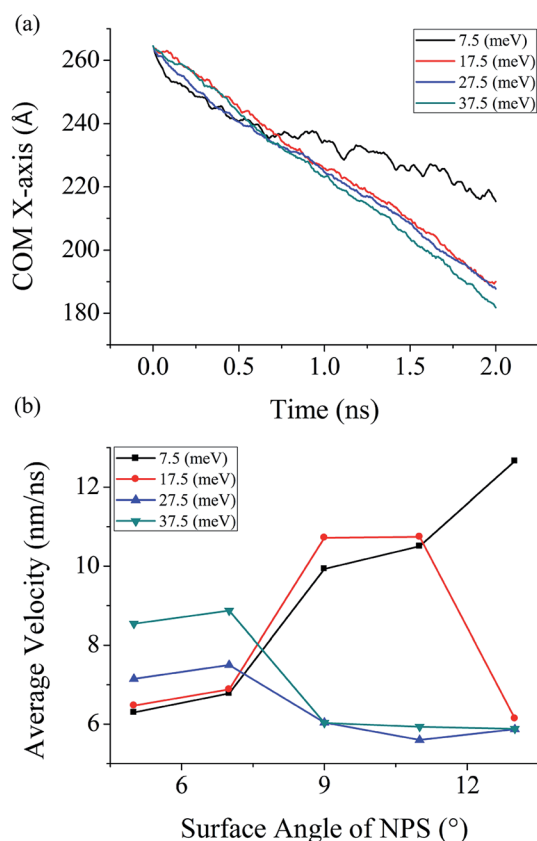
The Table 1 contains information about the water bridge formation on different types of NPS having different surface energy. It can be seen that there is no bridge formation in A5 in all cases except when the energy parameter is too low, *i.e.* 7.5 meV. In addition, there is no bridge formation in NPS having surface angle higher than 7° when the energy parameter is higher than 17.5 meV. Bridge formation is essential for efficient water transport, if there is no bridge formation then there will be no water transportation inside two NPSs. A detailed analysis on water bridge formation at NPS having different sizes of water droplet at different surface energy is listed in Table S2.†

In further analysis, the contact angle of water droplet on flat surface having variable surface wettability is conducted. In this study, a flat homogeneous surface constructed with same atomic lattice structure as that of NPS, is utilized. Its surface energy parameter is set equal to 7.5 meV, 17.5 meV, 27.5 meV, and 37.5 meV in order to observe the effect of surface wettability on the contact angle of water droplet. It was found that the contact angle of water droplet for each assigned energy parameter was calculated around 110.4°, 83.5°, 64.3°, and 40.2°, respectively.

The Fig. 7 exhibits that the water droplet started to spread on the solid surface when the energy parameter was increased to 37.5 meV. The contact angle of water droplet was around 110.5° when the energy parameter was 7.5 meV. It can be concluded that the surface with superhydrophilic characteristic is not suitable for this study as the contact angle of water will be too low, respectively, which will affect the bridge formation. These four energy parameter provides the information about the water surface contact angle which is essential information regarding bridge formation, if the water contact angle is too low then it will completely spread over the bottom surface and there will be no bridge formation and hence no water transportation will occur. In addition, if the water contact angle will be too high and the NPS is superhydrophobic it will be more efficient in bridge formation and could collect larger size of water droplet more easily. But this study is limited to analyze the water droplet transportation inside a NPS with surface wettability in moderate range, *i.e.* no superhydrophobic or superhydrophilic NPS is modelled. In addition, the influence of surface energy on the interaction energy between the solid–liquid surfaces is analyzed and listed in Table S3.†

Fig. 6 Simulated results of 4000 water molecules (a) COM data on A1 NPS (b) average velocity NPS with four different energy parameters.

Table 1 Table containing information about the effect of surface energy on water bridge formation between two NPSs containing 4000 molecules

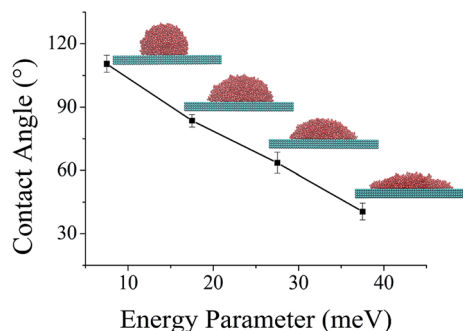| Surface energy (meV)	Type of NPS bridge formation (for 4000 water molecule droplet)				
	A1	A2	A3	A4	A5
7.5	Yes	Yes	Yes	Yes	Yes
17.5	Yes	Yes	Yes	Yes	No
27.5	Yes	Yes	No	No	No
37.5	Yes	Yes	No	No	No

Fig. 7 Simulated results of contact angle of 3000 water molecules after 1 ns simulation time on flat solid surface with four different assigned surface energy parameter.
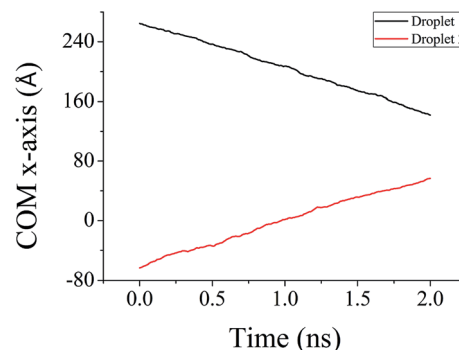

Fig. 9 Simulated results of COM data of two 4000 water molecules droplets over NPS along x-axis.

3.4 Unidirectional transport for large water droplet formation on multiple NPS

A unique design of NPS is proposed for collection of large size water droplets by combining two nanodroplets placed at each corner of the NPS. It is observed that the surface geometry plays a significant role in coalescence of two water droplets entrapped inside NPS. The NPS is designed in a manner to propel the water nanodroplets toward the center of the structure where they can coalesce and form a bigger size water droplet as shown in Fig. 8. This design is suitable for continuous water collection applications where large sized water droplets are desired.

The Fig. 8a exhibits the ensemble containing A3 (9°) NPS with two 4000 molecules water droplets placed at each corner of the NPS. Both droplets propel spontaneously towards the center of the NPS where they coalesce and form a bigger size water droplet as shown in Fig. 8e. The center of mass (COM) data is

also useful in understanding this transport and coalescence mechanism of two water droplets. As shown in Fig. 9a the COM data of both droplets along the x-axis is plotted and it can be seen that the droplets approach towards the center of the surface and the distance between the centers of each droplet is reduced by the course of simulation.

The COM data plotted in Fig. 9 shows that both droplets have almost similar rate of displacement and the plot converges by the passage of simulation time exhibiting that two droplets approach and coalesce with each other. The surface energy parameter for this case was set equal to 17.5 meV. These results further confirms that the surface geometry plays a significant role in pumpless transport of water droplet and such design features can be utilized for practical applications related to continuous water collection.

4. Conclusion

This simulation study provides a molecular level understanding about the unidirectional transport phenomena of water nanodroplet entrapped inside a nonparallel surface (NPS). It has been concluded that the A4 is most efficient among all the designed models when the water droplet is fixed at 6000 molecules with surface energy at 17.5 eV. In addition, the larger size droplets tend to move faster than the smaller size water nanodroplet. Moreover, the NPS with strong surface wettability, *i.e.* hydrophilic surface tends to induce faster droplet motion as compared to the hydrophobic NPS. The water bridge formation is essential for its transport and it does not occur when the surface angle is higher than 11°, except when the surface energy is 7.5 meV (hydrophobic) and has large water contact angle with the solid surface. The water bridge formation also does not occur in NPS having separation angle higher than 9° when the surface energy is 27.5 meV and 37.5 meV. The reason is related to the low water contact angle with the solid surface at high surface energy which results in no bridge formation hence there is no water transport in these cases. Furthermore, two water droplets were spontaneously transported and coalesced in a uniquely modeled design for practical applications which implies the significance of this work.
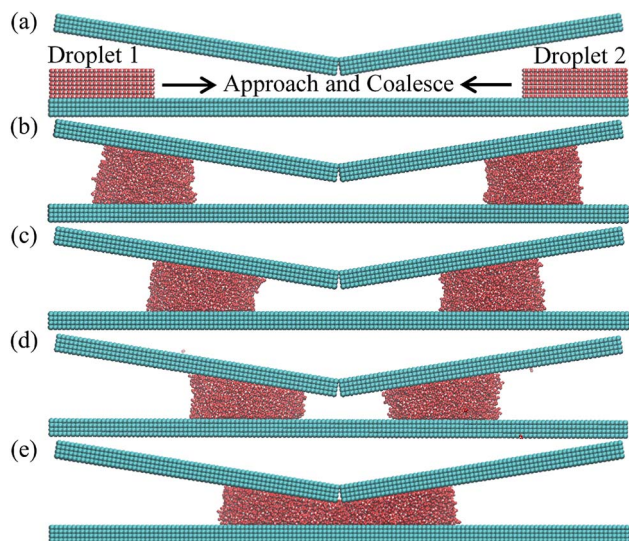

Fig. 8 Ensemble containing two 4000 molecules water nanodroplets placed inside each open end of 9° NPS exhibiting a larger water droplet formation (a) initial state (b) after 0.50 ns simulation time (c) after 1.0 ns simulation time (d) after 1.50 ns simulation time (e) after 2.0 ns simulation time or final state.

Conflicts of interest

The authors declare no competing financial interest.

Acknowledgements

References

1 F.-C. Wang, F. Yang and Y.-P. Zhao, Size effect on the coalescence-induced self-propelled droplet, *Appl. Phys. Lett.*, 2011, **98**(5), 053112.

2 N. Tretyakov and M. Müller, Directed transport of polymer drops on vibrating superhydrophobic substrates: a molecular dynamics study, *Soft Matter*, 2014, **10**(24), 4373–4386.

3 F. Mugele and J.-C. Baret, Electrowetting: from basics to applications, *J. Phys.: Condens. Matter*, 2005, **17**(28), R705.

4 J. Hong, J. K. Park, B. Koo, K. H. Kang and Y. K. Suh, Drop transport between two non-parallel plates *via* AC electrowetting-driven oscillation, *Sens. Actuators, B*, 2013, **188**, 637–643.

5 M. Becton and X. Wang, Thermal Gradients on Graphene to Drive Nanoflake Motion, *J. Chem. Theory Comput.*, 2014, **10**(2), 722–730.

6 J. Bennès, S. Alzuaga, P. Chabé, G. Morain, F. Chérioux, J. F. Manceau and F. Bastien, Action of low frequency vibration on liquid droplets and particles, *Ultrasonics*, 2006, **44**, e497–e502.

7 P. Hao, C. Lv, X. Zhang, Z. Yao and F. He, Driving liquid droplets on microstructured gradient surface by mechanical vibration, *Chem. Eng. Sci.*, 2011, **66**(10), 2118–2123.

8 A. Javadi, N. Moradi, V. B. Fainerman, H. Möhwald and R. Miller, Alkane vapor and surfactants co-adsorption on aqueous solution interfaces, *Colloids Surf., A*, 2011, **391**(1–3), 19–24.

9 S. De Luca, B. D. Todd, J. S. Hansen and P. J. Daivis, Molecular Dynamics Study of Nanoconfined Water Flow Driven by Rotating Electric Fields under Realistic Experimental Conditions, *Langmuir*, 2014, **30**(11), 3095–3109.

10 F. Dörfler, M. Rauscher, J. Koplik, J. Harting and S. Dietrich, Micro- and nanoscale fluid flow on chemical channels, *Soft Matter*, 2012, **8**(35), 9221–9234.

11 R. S. Subramanian, R. Shankar, N. Moumen and J. B. McLaughlin, Motion of a drop on a solid surface due to a wettability gradient, *Langmuir*, 2005, **21**(25), 11844–11849.

12 X. Zhu, H. Wang, Q. Liao, Y. D. Ding and Y. B. Gu, Experiments and analysis on self-motion behaviors of liquid droplets on gradient surfaces, *Exp. Therm. Fluid Sci.*, 2009, **33**(6), 947–954.

13 H. Chen, T. Tang and A. Amirfazli, Fast Liquid Transfer between Surfaces: Breakup of Stretched Liquid Bridges, *Langmuir*, 2015, **31**(42), 11470–11476.

14 H. Chen, T. Tang and A. Amirfazli, Liquid transfer mechanism between two surfaces and the role of contact angles, *Soft Matter*, 2014, **10**(15), 2503–2507.

15 M. A. Fortes, Axisymmetric liquid bridges between parallel plates, *J. Colloid Interface Sci.*, 1982, **88**(2), 338–352.

16 E. Buckingham, On Physically Similar Systems; Illustrations of the Use of Dimensional Equations, *Phys. Rev.*, 1914, **4**(4), 345–376.

17 M. Prakash, D. Quéré and J. W. M. Bush, Surface Tension Transport of Prey by Feeding Shorebirds: The Capillary Ratchet, *Science*, 2008, **320**(5878), 931.

18 C. Luo, X. Heng and M. Xiang, Behavior of a Liquid Drop between Two Nonparallel Plates, *Langmuir*, 2014, **30**(28), 8373–8380.

19 X. Heng and C. Luo, Bioinspired Plate-Based Fog Collectors, *ACS Appl. Mater. Interfaces*, 2014, **6**(18), 16257–16266.

20 R. Dangla, S. C. Kayi and C. N. Baroud, Droplet microfluidics driven by gradients of confinement, *Proc. Natl. Acad. Sci. U. S. A.*, 2013, **110**(3), 853.

21 W. Xu, Z. Lan, B. Peng, R. Wen, Y. Chen and X. Ma, Directional movement of droplets in grooves: suspended or immersed?, *Sci. Rep.*, 2016, **6**, 18836.

22 P. Concus and R. Finn, On The Behavior Of A Capillary Surface In A Wedge, *Proc. Natl. Acad. Sci. U. S. A.*, 1969, **63**(2), 292.

23 M. Ataei, H. Chen, T. Tang and A. Amirfazli, Stability of a liquid bridge between nonparallel hydrophilic surfaces, *J. Colloid Interface Sci.*, 2017, **492**, 207–217.

24 L. Wang, H. Wu and F. Wang, Efficient transport of droplet sandwiched between saw-tooth plates, *J. Colloid Interface Sci.*, 2016, **462**, 280–287.

25 B. Shi and V. K. Dhir, Molecular dynamics simulation of the contact angle of liquids on solid surfaces, *J. Chem. Phys.*, 2009, **130**(3), 034705.

26 C. W. Extrand, Contact Angles and Hysteresis on Surfaces with Chemically Heterogeneous Islands, *Langmuir*, 2003, **19**(9), 3793–3796.

27 S. Chen, J. Wang and D. Chen, States of a Water Droplet on Nanostructured Surfaces, *J. Phys. Chem. C*, 2014, **118**(32), 18529–18536.

28 C. Lv, C. Chen, Y.-C. Chuang, F.-G. Tseng, Y. Yin, F. Grey and Q. Zheng, Substrate Curvature Gradient Drives Rapid Droplet Motion, *Phys. Rev. Lett.*, 2014, **113**(2), 026101.

29 S. Chen, J. Wang and D. Chen, Wetting Behaviors of an Underwater Oil Droplet on Structured Surfaces, *MRS Adv.*, 2016, **1**(10), 667–673.

30 H. J. C. Berendsen, J. R. Grigera and T. P. Straatsma, The missing term in effective pair potentials, *J. Phys. Chem.*, 1987, **91**(24), 6269–6271.

31 S. Do Hong, M. Y. Ha and S. Balachandar, Static and dynamic contact angles of water droplet on a solid surface

using molecular dynamics simulation, *J. Colloid Interface Sci.*, 2009, **339**(1), 187–195.

32 C. D. Daub, J. Wang, S. Kudesia, D. Bratko and A. Luzar, The influence of molecular-scale roughness on the surface spreading of an aqueous nanodrop, *Faraday Discuss.*, 2010, **146**, 67–77.

33 Z. Zhang, H. Kim, M. Y. Ha and J. Jang, Molecular dynamics study on the wettability of a hydrophobic surface textured with nanoscale pillars, *Phys. Chem. Chem. Phys.*, 2014, **16**(12), 5613–5621.

34 H. J. C. Berendsen, J. P. M. v. Postma, W. F. van Gunsteren, A. DiNola and J. R. Haak, Molecular dynamics with coupling to an external bath, *J. Chem. Phys.*, 1984, **81**(8), 3684–3690.

35 C. M. Care and D. J. Cleaver, Computer simulation of liquid crystals, *Rep. Prog. Phys.*, 2005, **68**(11), 2665.

36 S. Plimpton, Fast parallel algorithms for short-range molecular dynamics, *J. Comput. Phys.*, 1995, **117**(1), 1–19.

37 S. Muhammad and F. Ebrahimi, Efficient Transport Between Disjoint Nanochannels by a Water Bridge, *Phys. Rev. Lett.*, 2019, **122**(21), 214506.